

MODELING OF THE EVOLUTION OF THE OPTICAL, RADIATIVE AND THERMODYNAMIC CHARACTERISTICS OF THE ATMOSPHERE DURING CRYSTALLIZATION OF CLOUDS. I. COMPLETE DISPERSAL OF CLOUDS

K.A. Kondrat'ev, M.V. Ovchinnikov, and V.I. Khvorost'yanov

*Institute of Limnology
of the Academy of Sciences of the USSR, Leningrad and
Central Aerological Observatory, Dolgoprudnyi
Received November 20, 1989*

The interaction of the radiation fields with the microphysical and dynamical characteristics of clouds under conditions of artificial crystallization and complete dispersal of the clouds is investigated based on a two-dimensional mesoscale numerical model of cloud formation and precipitation developed by the authors (pp. 639–646 of this issue). Analysis of the results of the numerical experiment confirms the possibility that the optical, radiation, and thermodynamic parameters of the atmospheric boundary layer can be changed substantially in the case of artificial dispersal of the clouds, i.e., local change in the optical weather.

During the last decade, in addition to the continuing traditional investigations in the physics of the atmosphere, increasing attention is being devoted to the possibility of weather modification.^{1,2,3,4} Because the radiation balance at the earth's surface and the diurnal behavior of the temperature depend on the presence of clouds and fog (the greenhouse and antigreenhouse effects), there arises the possibility of modifying the weather by means of artificial dispersal of clouds and fogs. The first practical works along these lines were performed in the middle of this century.^{1,2}

An appreciable increase in the daytime temperature as a result of artificial dispersal of clouds and fogs can be achieved only for positive values of the radiation balance under cloud-free conditions. During the winter months, in the period when supercooled clouds, suitable for seeding for purposes of dispersal, appear most often, this condition is observed only in the southern regions of the USSR, while during the transitional seasons it appears in almost all regions. On January 12, 1961 V.V. Vyal'tsev and N.V. Volovikov performed in the region of the town of Nal'chik an experiment in which the daytime temperature at the ground was increased by 5–7°C by means of artificial dispersal of fog owing to a reduction of the albedo of the fog-underlying surface system.¹

Over the last ten years the most significant investigations on cloud dispersal were performed over Moscow on December 7, 1986 by researchers at the Central Aerological Observatory. A detailed account of the results of this experiment is given in Ref. 3.

Cloud dispersal and perturbation of meteorological elements are always connected, one way or another, with significant changes in the optical and

radiation characteristics of the atmosphere, which in aggregate are referred to by the term "optical weather".⁵ Thus when clouds are seeded in order to disperse them one can talk not only about weather modification in the meteorological sense but also about the modification of the optical weather. The latter aspect can be of great practical value in the process of wide introduction of different optical systems in the national economy.⁵

In spite of the quite extensive experience accumulated on weather modification, however, our knowledge of seeding and processes occurring in the zone of seeding is incomplete. This is attributable primarily to the difficulty of remote monitoring of the effect of seeding as well as to the fact that the high cost of experiments limits the number of experiments that can be performed under different meteorological conditions in order to obtain statistically well-founded results. Thus it is desirable to perform investigations with the help of numerical simulation of atmospheric processes occurring during optical weather modification. For this it is especially important to formulate models with a minimum number of simplifications and parameterizations.

In Ref. 6 we described a two-dimensional mesoscale numerical model of cloud formation and precipitation. This model enables investigation of the interaction of radiation fields with the microphysical and dynamical characteristics of clouds during artificial crystallization and dispersal of the clouds. This paper is devoted to the analysis of the results of numerical experiments based on this model.

Before we proceed to describe the seeding process, we shall examine briefly the processes in the model that lead to cloud formation. The initial time

corresponds to 01:00 in the morning and there are no clouds. The effective long-wave length emission of the earth's surface, which at this time is equal to 76 W/m^2 , results in a decrease of the temperature at the surface from 0°C to -3°C within the first two hours. The decrease in the temperature then slows down; this is explained primarily by the turbulent flow of heat from the atmosphere to the surface, which partially compensates the emission of the surface, and partially by the flow of heat from deep within the soil. Over the next two hours the decrease in temperature already does not exceed 1°C . The flux of latent heat $B_Q = L_q \rho_a \partial q / \partial z$, (where q is the moisture content, z is the altitude, ρ_a is the density of air, and L_q is the specific heat of condensation), which accompanies condensation of vapor from the atmosphere on the surface, also makes a definite contribution to the retardation of the cooling. But this flux is relatively small and does not exceed 5 W/m^2 . The rate of efflux of vapor is less than the rate of radiation cooling, and for this reason in spite of the fact that the specific moisture content decreases the undersaturation (dew-point deficit) decreases.

The process described leads to the fact that after 3.5 h of natural evolution the undersaturation is zero (the relative moisture content is equal to 100%), and condensation of vapor and formation of a low cloud starts. By 06:00 there forms a stable cloud with boundaries at altitudes of 100 and 900 m and with maxima liquid-water content of 0.15 g/kg at an altitude of 750 m. At this time the sun rises. In the model the latitude of the location was taken to be $\varphi = 56^\circ$ (the latitude of Moscow) and the angle of inclination of the sun $\delta = 0^\circ$, which corresponds to the equinox (March 21), at which the sun rises at 06:00 and sets at 18:00.

At this time of year at the given latitude supercooled clouds most likely appear above an already show-free underlying surface, i.e., above a surface with a low albedo ($A_s = 0.35$). Starting the seeding soon after sunrise makes it possible to obtain estimates of the maximum possible perturbations of the thermodynamic, radiation, and optical characteristics of clouds during crystallization, since the values of such disturbances are determined primarily by the length of time the seeded zone is exposed to sunlight. The initial time (01:00) was chosen so that the cloud would evolve into a stable formation by sunrise.

There is no crystalline phase before the reagent is introduced. Seeding starts at 07:00. Periodic seeding with solid granules of carbonic acid at an altitude of 1100 m was modeled (i.e., 100 to 200 m above the top boundary of the cloud).

The physical aspect of the seeding is as follows. A particle of solid carbonic acid is introduced into the air, which is strongly cooled as the particle evaporates. The cooling is the main reason for the supersaturation of water vapor. This supersaturation can be so significant that it exceeds the critical value required for formation of drops and ice crystals di-

rectly on complexes of water molecules (homogeneous condensation and crystallization). At a temperatures of -40°C and lower stable ice nuclei form from the complexes of water molecules. The number of ice crystals N , forming as a result of the evaporation of 1 g of solid carbonic acid, dumped into the cloud, was measured under laboratory conditions and ranges from $5 \cdot 10^{11}$ to $1.2 \cdot 10^{14}$ depending on the temperature of the surrounding air.⁷ As the temperature decreases N increases. In the model the described process of nucleation of crystals was not calculated in order to save time, and the seeding was modeled by introducing at the nodes of the difference grid ($x = 10 \text{ km}$, $z = 200\text{--}1100 \text{ m}$) a definite number of crystals (the concentration of crystals $P_{cr} = 1000 \text{ g}^{-1}$) every 10 min (seeding). This corresponds to the aircraft flying past the point with coordinates $x = 10 \text{ km}$, $z = 1100 \text{ m}$ perpendicular to the $x - z$ plane and, correspondingly, perpendicular to the flow (since the geostrophic wind is directed along the x -axis). Assuming that when 1 g of solid carbonic acid evaporates 10^{12} ice crystals form and that the granules completely evaporate over a distance of the order of 1 km, the indicated concentration of crystals introduced corresponds to the consumption of -1 kg of reagent per 1 km of the flight path.

When the crystals enter the supercooled droplet cloud the following happens (by "supercooled" we mean a droplet cloud existing at negative temperature). In the steady-state cloud the supersaturation of the vapor above the water Δ_1 is practically equal to zero, but the supersaturation above ice Δ_2 is positive. Thus crystals start to grow, and this results in a decrease of Δ_1 and Δ_2 owing to sublimation of the vapor; in addition, Δ_1 becomes negative (undersaturation is observed above water). But for $\Delta_1 < 0$ vapor starts to evaporate from the drops. The process described above is called "transfer" of vapor from drops to crystals.⁷

If there are not too many crystals, then they grow to sizes sufficient for precipitation in the form of snow. Thus we have achieved a reduction of the concentration of drops as a result of their evaporation (in the limit, with a corresponding number of crystals, i.e., with the corresponding dose of the reagent, to zero), and a reduction of the concentration of crystals (in the limit also to zero) owing to their precipitation. This is the principle for dispersing supercooled clouds by the method of artificial crystallization of the clouds.

We shall examine the evolution of seeding zone. Already one hour after the start of seeding the liquid water in the central part disappears owing to transfer of vapor from drops to crystals, i.e., in this zone the cloud crystallizes completely. Later the following stable picture forms (see Fig. 1). The cloud disperses downstream (to the right in Fig. 1) from the line of seeding. At first it crystallizes completely over a distance of 5–8 km (Fig. 1b), and then over a distance of 15–20 km both the liquid water and the ice vanish owing to the precipitation of crystals. Compar-

ing Figs. 1a and 1b shows that the ice content of the crystallized cloud decreases along the flow more slowly than the concentration. This is connected primarily with an increase in the size of the crystals. Spreading along the flow, they grow quite rapidly and precipitate out. In the process, their concentration decreases significantly (Fig. 1a).

In Fig. 1c one can see that the local meteorological visibility range⁶ is sharply higher to the right of the line of seeding. It should be noted that this increase occurs significantly more rapidly than the cloud disperses (in the sense that the liquid water and ice in the cloud vanish). The point is that the crystallized cloud is more transparent than a droplet cloud owing to the lower concentration of particles. Thus considering two regions with the same total water content in the droplet and crystalline parts of the cloud (for example, isolines with $q_{L1,2} = 0.10$ g/kg in Fig. 1b), it is obvious that in the first case the visibility range $L = 0.34$ km while in the second case $L = 1.94$ km, i.e., it is almost six times longer. Ten to 15 km from the line of seeding the visibility range already exceeds 5 km.

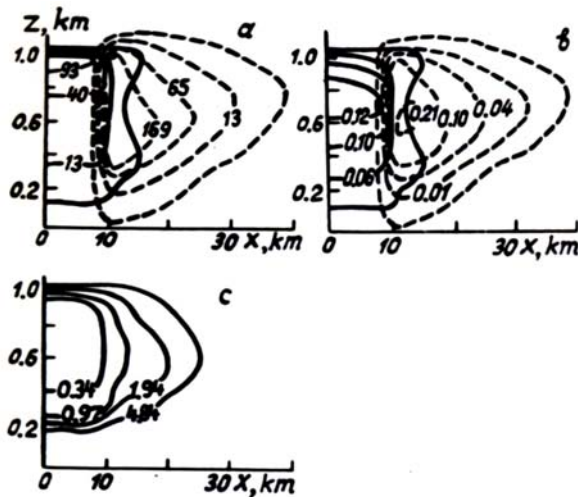


FIG. 1. Two-dimensional fields of microphysical parameters of the droplet (solid curves) and crystalline (dashed curves) phases and the visibility range $L = 7$ h after seeding starts (the concentration of droplets, N_1 , in 10^3 g^{-1} and concentration of crystals N_2 , in g^{-1} (a); the liquid water content q_{L1} , in g/kg , the ice content q_{L2} , in g/kg (b); and, L , km (c)).

We note that all two-dimensional fields (Figs. 1, 2, 3, and 4) are given at times when the temperature perturbation is maximum, i.e., at 14:00.

Figure 2 shows the radiation characteristics of the short-wavelength radiation (SWR). There are the upward and downward fluxes, the Influx or rate of radiation-induced change in the temperature, and the albedo. It is obvious that changes in the microphysical parameters also result in significant transformation of the radiation characteristics. Thus when the downward flux of solar radiation (Fig. 2b) passes through a droplet cloud it is attenuated by more than a factor of two, decreasing from

$591 \text{ W}/\text{m}^2$ at an altitude of 1 km to $270 \text{ W}/\text{m}^2$ at an altitude of 0.3 km. In the crystallization zone this attenuation is no longer so significant and does not exceed 20% (591 and $500 \text{ W}/\text{m}^2$, respectively). The albedo also changes just as significantly: from 63% above the flowing cloud up to 41% above the crystallization zone and then to the albedo of the underlying surface $A_s = 35\%$. In addition, examining the albedo of the cloud itself, i.e., the quantity $A - A_s$, we see that it changes almost by a factor of five from 28% to 6%, while the influx in the indicated regions differs by only a factor of 2.5 (0.51 and $0.21^\circ\text{C}/\text{h}$, respectively).

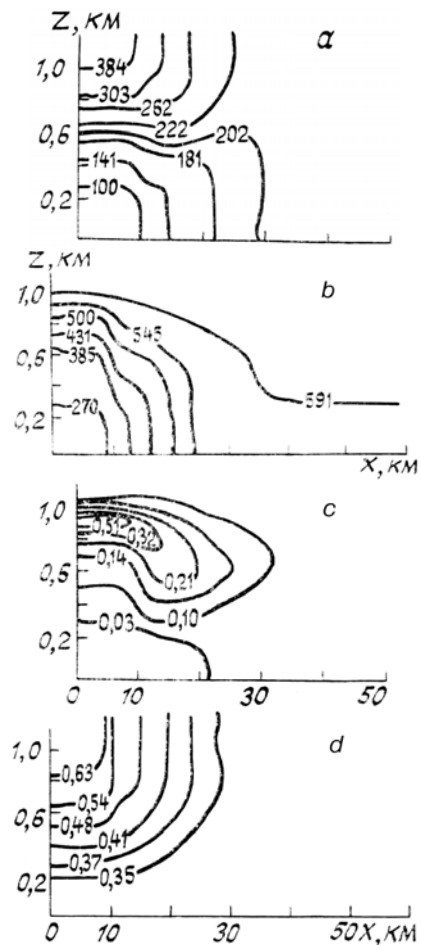


FIG. 2. A vertical section of the fields of the solar radiation characteristics: (a) upward F_s^{\uparrow} , in W/m^2 , flux and downward F_s^{\downarrow} , in W/m^2 , (b), flux and the the influx $(\partial T/\partial t)_s$, in $^\circ\text{C}/\text{h}$, (c) of solar radiation and the albedo field A , (d).

The indicated more rapid decrease (in the process of crystallization and with growth of crystals the albedo) than the absorption is studied in greater detail in Refs. 8 and 9. In the cleared zone the downward and upward fluxes of solar radiation do not change significantly and their values at the underlying surface are close to the values at an altitude of 1 km. The insignificant decrease in the downward

flux is due to the absorption by water vapor. The screening of the solar radiation by the cloud, as is observed for small values of x , is not observed here. For this reason, in particular, the downward flux at the ground in the cleared zone is significantly higher than at the same level above the cloud (Fig. 2b). Such a strong change ($F_s^\downarrow = 270 \text{ W/m}^2$ at a height of 300 m beneath the cloud, while in the cleared zone $F_s^\downarrow = 591 \text{ W/m}^2$ at the same height) over a distance of 20–25 km gives rise to a sharp contrast in the radiation balance at the ground, which in turn gives rise to nonuniform perturbations of the temperature, which will be examined below.

Figure 3 shows the upward (a) and downward (b) fluxes of the long-wavelength radiation (LWR) as well as the rate of radiat ion-induced change in the temperature $(\partial T/\partial t)_1$ owing to the influx of LWR (c). The well-known cooling occurs at the top of the cloud (Fig. 3c), and reaches a magnitude of 2.2°C/h (because it is localized in a very narrow region this isoline is not shown in Fig. 3c). The effective emission of the winter surface, which determines the upward flux of LWR, is appreciably screened by the clouds. Thus in the cleared zone $F_1^\uparrow = 306 \text{ W/m}^2$ at an altitude of 1 km, while above the cloud $F_1^\uparrow = 273 \text{ W/m}^2$. The difference in the upward fluxes at the ground is explained by the non-uniformity of the surface temperature. Below the cloud, where the ground temperature is equal to 6.5°C , the upward flux is equal to 348 W/m^2 , and at locations where the cloud has dispersed, the ground temperature exceeds 13.4°C and, correspondingly, the upward flux of LWR is larger -382 W/m^2 (Fig. 3a).

Figure 4 shows the temperature field and the field of the coefficient of turbulence. The temperature at the surface rises continuously over a distance of 25 km from 6.5°C beneath the cloud to 13.4°C in the cleared zone (Fig. 4a), after which it remains virtually constant. Under the conditions studied the temperature disturbances are appreciable not only at the surface but also at altitudes up to 1 km. Thus the indicated disturbance is equal to approximately 6°C at an altitude of 200 m and 4°C at an altitude of 500 m, and a significant disturbance of the temperature (up to 2°C) is observed even an altitude of 800 m in the cleared zone compared with the cloud-covered zone. The temperature is horizontally uniform only at altitudes above 1 km.

Above the zone of enhanced heating, somewhat downstream, significant turbulence is observed (Fig. 4b). The reason for this is that the heating of the bottom air layers intensifies the instability of the thermal stratification, which results in an intensification of turbulence. The increase in the turbulence coefficient K at altitudes from 50 to 200 m by at least a factor of 1.5 (from $20 \text{ m}^2/\text{sec}$ at an altitude of 50 m to $30\text{--}35 \text{ m}^2/\text{sec}$ at altitudes of 150–200 m) encourages the thermal disturbance to spread out vertically.

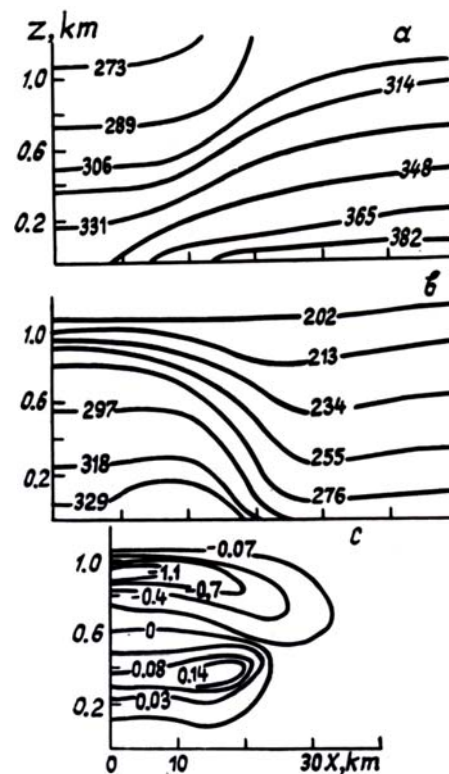


FIG. 3. A vertical section of the fields of the characteristics of LWR: (a) upward flux F_1^\uparrow , in W/m^2 ; downward flux F_1^\downarrow , in W/m^2 ; (b) and, (c) the influx $(\partial T/\partial t)_1$, in $^\circ\text{C/h}$.

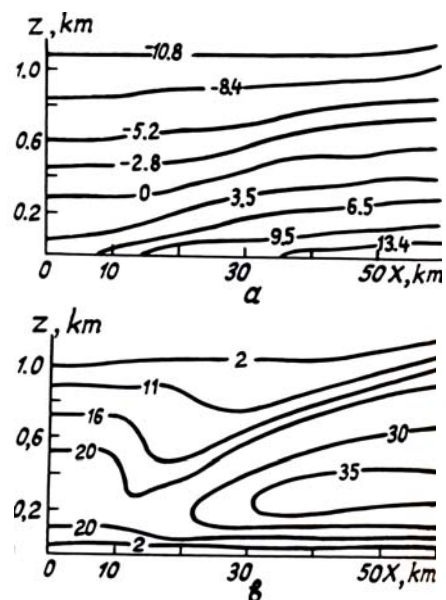


FIG. 4. A vertical section of the temperature field T (in $^\circ\text{C}$) (a) and the field of the turbulence coefficient K (in m^2/sec) (b) seven hours after seeding starts.

The computational results presented in this part of the work indicate that significant changes in the

optical, radiation, and thermodynamic characteristics of the atmospheric boundary layer can be achieved by artificial crystallization of clouds in the case of cloud dispersal. Thus the numerical experiment performed has confirmed the fact that it is in principle possible to modify the optical weather by means of artificial dispersal of clouds. In Part 2 of this work we shall describe a case when reformation of clouds after dispersal prevents the realization of the possibility indicated in this paper.

REFERENCES

1. V.I. Belyaev, V.V. Vyal'tsev, and I.S. Pavlova, *Izv. Akad. Nauk SSSR, Ser. FAO* **2**, No. 6, 630–635 (1966).
2. A. Dennis, *Weather Modification by Cloud Seeding* [Russian translation], Mir, Moscow (1983).
3. G.P. Berjulev, I.I. Burtsev, N.K. Vinnichenko, et al., *Meteorolog. Gidrolog.*, No. 12, 38–48 (1988).
4. V.I. Khvorost'yanov and A.M. Yudov, in: *Tr. TsAO, Leningrad* (1986), No. 162, pp. 63–76.
5. B.D. Belan and G.O. Zadde, *Forecasting and Monitoring of the Optical and Meteorological State of the Atmosphere* [in Russian], Tomsk Affiliate of the Siberian Branch of the Academy of Sciences of the USSR, Tomsk (1982).
6. K.Ya. Kondrat'yev, M.V. Ovchinnikov and V.I. Khvorost'yanov, *Opt. Atmos.* **3**, No. 6, 639–646 (1990).
7. L.T. Matveev, *A Course in General Meteorology Physics of the Atmosphere* [in Russian], Gidrometeoizdat, Leningrad (1984), 751 pp.
8. K.Ya. Kondrat'yev, M.V. Ovchinnikov, and V.I. Khvorost'yanov, *Opt. Atmos.* **1**, No. 6, 57–66 and No. 7, pp. 98–105 (1988).
9. K.Ya. Kondrat'yev, V.I. Khvorost'yanov, and M.V. Ovchinnikov, in: *Proceeding of the Tenth International Symposium on the Atmospheric Radiation*, Lille, France (1988), pp. 71–72.